THE JOURNAL OF BIOLOGICAL CHEMISTRY
Vol. 275, No. 20, Issue of May 19, pp. 15265–15270, 2000

Printed in U.S.A.

Binding of Alkylurea Inhibitors to Epoxide Hydrolase Implicates Active Site Tyrosines in Substrate Activation*

Received for publication, January 11, 2000, and in revised form, March 8, 2000
Published, JBC Papers in Press, March 9, 2000, DOI 10.1074/jbc.M000278200

Maria A. Argiriadi‡§, Christophe Morisseau¶, Marvin H. Goodrow¶, Deanna L. Dowdy¶, Bruce D. Hammock¶, and David W. Christianson‡‖

From the ‡Roy and Diana Vagelos Laboratories, Department of Chemistry, University of Pennsylvania, Philadelphia, Pennsylvania 19104-6323 and the ¶Department of Entomology, University of California, Davis, California 95616

The structures of two alkylurea inhibitors complexed with murine soluble epoxide hydrolase have been determined by x-ray crystallographic methods. The alkyl substituents of each inhibitor make extensive hydrophobic contacts in the soluble epoxide hydrolase active site, and each urea carbonyl oxygen accepts hydrogen bonds from the phenolic hydroxyl groups of Tyr^{381} and Tyr^{465}. These hydrogen bond interactions suggest that Tyr^{381} and/or Tyr^{465} are general acid catalysts that facilitate epoxide ring opening in the first step of the hydrolysis reaction; Tyr^{465} is highly conserved among all epoxide hydrolases, and Tyr^{381} is conserved among the soluble epoxide hydrolases. In one enzyme-inhibitor complex, the urea carbonyl oxygen additionally interacts with Gln^{382}. If a comparable interaction occurs in catalysis, then Gln^{382} may provide electrostatic stabilization of partial negative charge on the epoxide oxygen. The carboxylate side chain of Asp^{333} accepts a hydrogen bond from one of the urea NH groups in each enzyme-inhibitor complex. Because Asp^{333} is the catalytic nucleophile, its interaction with the partial positive charge on the urea NH group mimics its approach toward the partial positive charge on the electrophilic carbon of an epoxide substrate. Accordingly, alkylurea inhibitors mimic features encountered in the reaction coordinate of epoxide ring opening, and a structure-based mechanism is proposed for leukotoxin epoxide hydrolysis.

Epoxide hydrolases catalyze epoxide ring opening to produce 1,2-diol products (1, 2). In mammals, these enzymes exist in two major forms: soluble epoxide hydrolase (sEH),[1] which is found in the cytosol and peroxisomal matrix, and microsomal epoxide hydrolase, which is membrane-anchored (1, 3, 4). Both sEH and microsomal epoxide hydrolase are involved in the metabolism of numerous xenobiotics, and sEH also plays a crucial role in lipid epoxide homeostasis. For example, sEH catalyzes the hydrolysis of *cis*-9,10-epoxyoctadec-9(Z)-enoic acid (leukotoxin) to form its corresponding diol, *threo*-9,10-dihydroxyoctadec-12(Z)-enoic acid (leukotoxin diol), and sEH similarly catalyzes the hydrolysis of *cis*-12,13-epoxyoctadec-9(Z)-enoic acid (isoleukotoxin) to form its corresponding diol *threo*-12,13-dihydroxyoctadec-9(Z)-enoic acid (isoleukotoxin diol) (5) (Fig. 1). Leukotoxins can perturb membrane permeability and ion transport and cause inflammatory responses (5, 6). Accordingly, sEH is a possible pharmaceutical target for the treatment of acute disorders such as multiple organ failure and adult respiratory distress syndrome (7).

Recently, the crystal structure of native sEH was reported at 2.8 Å resolution (8). The enzyme adopts a homodimeric, domain-swapped architecture in which the C-terminal domain belongs to the α/β hydrolase fold family (9, 10). The C-terminal domain, or "catalytic domain," contains the active site residues required for epoxide hydrolysis. By analogy with related α/β hydrolases such as haloalkane dehalogenase (11–13) and in accord with labeling (14) and site-directed mutagenesis experiments (15, 16), Asp^{333} is the catalytic nucleophile that attacks the epoxide carbon in the first step of sEH catalysis. Asp^{333} hydrogen bonds to His^{523}, and this interaction may help to stabilize Asp^{333} in the ionization state required for catalysis. The side chain of Asp^{495} is close to His^{523}, and a hydrogen bond may form between these two residues during catalysis. Given its active site location and absolute conservation among all sequenced epoxide hydrolases, Tyr^{465} is a likely general acid that donates a proton to the epoxide oxygen in the first step of catalysis (8, 17). The structure of native sEH also reveals that Tyr^{381} is similarly located in the active site; being conserved among the sEH enzymes, this residue is likewise a candidate general acid (8, 17). However, because Tyr^{381} is not universally conserved among all epoxide hydrolases (it is apparently absent from the microsomal enzymes), it cannot be a universal general acid. The active site tunnel is L-shaped, with catalytic residues located at the corner of the L. Both ends of the L open to solvent; one end consists of a long, narrow hydrophobic channel, and the other end consists of a shorter, wider cleft containing a hydrophobic pocket. Although the N-terminal domain of sEH resembles other hydrolytic enzymes such as haloacid dehalogenase (18, 19), this domain does not participate in epoxide hydrolysis, even though it contains an intact active site (8).

Although the structures of native sEH enzymes from *Agrobacterium radiobacter* AD1 (17), *Aspergillus niger* (20), and murine (8) sources are reported, no structural information is available regarding inhibitor binding to the sEH active site

* This work was supported by National Institutes of Health Grant GM56838 and NIEHS, National Institutes of Health Grants 2 R01 ES02710-16 and 2 P42 ES0469909. University of California, Davis, is supported in part by NIEHS Health Sciences Center Grant 1 P30 ES05707-04. The costs of publication of this article were defrayed in part by the payment of page charges. This article must therefore be hereby marked "*advertisement*" in accordance with 18 U.S.C. Section 1734 solely to indicate this fact.

The atomic coordinates of epoxide hydrolase-inhibitor complexes have been deposited in the Research Collaboratory for Structural Bioinformatics with accession codes 1EK1 and 1EK2.

§ Supported in part by the University of Pennsylvania Plant Sciences Training Grant and the Nicholas Padis Graduate Fellowship from the Hellenic University Club of Philadelphia.

‖ To whom correspondence should be addressed. Tel.: 215-898-5714; Fax: 215-573-2201; E-mail: chris@xtal.chem.upenn.edu.

[1] The abbreviations used are: sEH, soluble epoxide hydrolase; mEH, microsomal epoxide hydrolase; CPU, *N*-cyclohexyl-*N*′-(3-phenylpropyl)urea; CDU, *N*-cyclohexyl-*N*′-decylurea; CIU, *N*-cyclohexyl-*N*′-(4-iodophenyl)urea; r.m.s., root mean square.

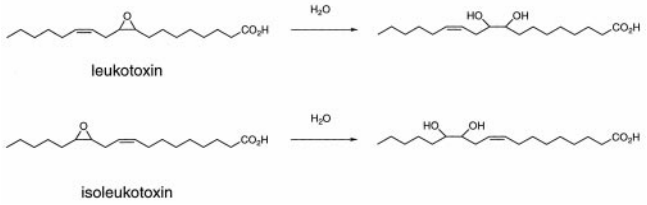

FIG. 1. **Leukotoxin hydrolysis reaction catalyzed by sEH.**

except for a single murine sEH-dialkylurea inhibitor complex (8). Dialkylureas are potent inhibitors of the recombinant murine and human enzymes (7), and the crystal structure of the murine sEH-*N*-*cyclohexyl*-*N*′-(3-phenyl)propylurea (CPU; K_i = 3.1 nM) complex reveals an unusual *trans, cis*-conformation for the dialkylurea moiety; inhibitor binding is stabilized by numerous hydrophobic van der Waals' contacts and a single hydrogen bond between Tyr^{465} and a urea NH group (8). Although the structure of the sEH-CPU complex confirmed the location of the sEH active site, it did not provide meaningful clues about substrate or transition state binding; the polarity of the single enzyme-inhibitor hydrogen bond was inconsistent with a potential function for Tyr^{465} as a catalytic proton donor, and the known catalytic nucleophile Asp^{333} did not contact the inhibitor. Thus, the mechanistic inferences from the first and only available structure of an sEH-inhibitor complex were quite limited. Could Tyr^{381} or other polar residues in the sEH active site participate in inhibitor and/or substrate binding?

To clarify mechanistic inferences from the binding of potent alkylurea inhibitors to sEH, we now report the x-ray crystal structure determinations of sEH complexed with two different inhibitors: *N*-cyclohexyl-*N*′-decylurea (CDU; $K_i = 6.3 \pm 0.5$ nM) and *N*-cyclohexyl-*N*′-(4-iodophenyl)urea (CIU; $K_i = 17 \pm 4$ nM) (Fig. 2). These inhibitors bind in the sEH active site and directly mimic interactions consistent with the activation of a substrate epoxide ring for nucleophilic attack by Asp^{333}.

EXPERIMENTAL PROCEDURES

Inhibitor Syntheses—To a stirred solution of 0.60 ml (0.47 g, 3.0 mmol) of decylamine in 20 ml of hexane was added 0.38 ml (0.37 g, 3.0 mmol) of cyclohexylisocyanate, which produced a white crystalline solid. After standing overnight the mixture was cooled, and the solid product was collected, washed with cold hexane, and dried to obtain 0.776 g (2.75 mmol, 92%) of CDU as a white powder, mp 88.5–89.5 °C: IR (KBr) 3345 (m, NH), 3318 (m, NH), 1624 (*versus*, C=O), 1578 (s, amide II) cm^{-1}; ^1H NMR (300.1 MHz, $CDCl_3$) δ 4.2 (m, 2 H, 2 NH), 3.5 (m, 1 H, CH-1), 3.13 (dt, J = 6.0, 6.8 Hz, 2 H, CH_2-1′), 1.9 (m, 2 H), 1.0–1.8 (m, 24 H), 0.88 (t, J = 6.9 Hz, 3 H, CH_3); ^{13}C NMR (75.5 MHz, $CDCl_3$) δ 158.3 (C=O), 48.7 (C-1), 40.4 (C-1′), 34.0 (C-2, 6), 31.8 (C-6′), 30.4 (C-2′), 29.6 (C-7′, 8′), 29.4 (C-4′), 29.3 (C-5′), 27.0 (C-3′), 25.6 (C-4), 25.0 (C-3, 5), 22.6 (C-9′), 14.0 (C-10′); fast atom bombardment-mass spectrum *m/z* (relative intensity) 284 (22, M + H^+ +1), 283 (100, M + H^+); Atmospheric Pressure Chemical Ionization-HRMS *m/z* calculated for $C_{17}H_{35}N_2O$ [M + H^+] 283.2749, observed 283.2751. Inhibition of sEH was assayed as described (7), yielding $K_i = 6.3 \pm 0.5$ nM.

A solution of 1.10 g (5.00 mmol) of 4-iodoaniline and 0.688 g (5.50 mmol) of cyclohexylisocyanate in 25 ml of ether kept in the dark at ambient temperature, deposited 0.591 g of CIU after 1 week. Recrystallization of the solid from methanol after treatment with Norite produced 0.332 g (20%) of white needles, mp 246.5–247.5 °C. After one month, the above filtrate, when evaporated to dryness, and the residue recrystallized from ethanol provided another 0.580 g of product as white needles, mp 246.5–247.5 °C, for a total yield of 55%. TLC (0.2-mm silica gel 60 F254 on plastic sheets from E. Merck) R_f 0.38 (tetrahydrofuran/ethyl acetate/hexane, 2:13:35, v/v/v); IR (KBr) 3343 (m, NH), 3280 (m, NH), 1631 (*versus*, C=O), 1558 (s, amide II) cm^{-1}; ^1H NMR (300.1 MHz, Me_2SO-d_6) δ 8.39 (s, 1 H, ArNH), 7.50 (d, J = 8.7 Hz, 2 H, ArH-3, 5), 7.21 (d, J = 8.7 Hz, ArH-2, 6), 6.08 (d, J = 7.5 Hz, 1 H, NH), 3.4 (m, 1 H, CH), 1.8 (m, 2 H), 1.6 (m, 2 H), 1.5 (m, 1 H), 1.2 (m, 5 H); ^{13}C NMR (75.5 MHz, Me_2SO-d_6) δ 154.3 (C=O), 140.6 (ArC-1), 137.2 (ArC-3, 5), 120.0 (ArC-2, 6), 83.3 (ArC-4), 47.7 (C-1), 33.0 (C-2, 6), 25.3 (C-4), 24.4 (C-3, 5); fast atom bombardment-mass spectrum *m/z* (relative intensity) 346 (17, M + H^+ + 1), 345 (100, M + H^+); Atmospheric Pressure Chemical Ionization-HRMS *m/z* calculated for $C_{13}H_{18}IN_2O$ [M + H^+] 345.0464, observed 345.0449. Inhibition of sEH was assayed as described (7), yielding $K_i = 17 \pm 4$ nM.

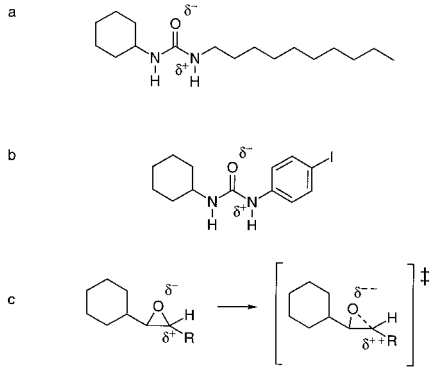

FIG. 2. **Disubstituted cyclohexyl ureas.** *a*, *N*-cyclohexyl-*N*′-decylurea; *b*, *N*-cyclohexyl-*N*′-(4-iodophenyl)urea. Note that the urea moiety mimics structural and electrostatic features along the reaction coordinate of epoxide ring opening (*c*).

TABLE I
Data collection and refinement statistics for sEH-CDU and sEH-CIU complexes

	CDU	CIU
Number of measured reflections	46,217	73,240
Number of unique reflections	19,689	19,761
Maximum resolution (Å)	3.0	3.1
R_{merge} [a]	0.069	0.110
Completeness of data (%)	79.4	89.6
Number of reflections used in refinement (>2 σ)	18,059	18,197
Number of reflections in R_{free} test set	924	933
R_{cryst} [b]	0.211	0.194
R_{free} [b]	0.290	0.305
Number of non-hydrogen atoms	8,218	8,212
Number of solvent molecules included in refinement	19	21
r.m.s. deviation from ideal bond lengths (Å)	0.007	0.017
r.m.s. deviation from ideal bond angles (°)	1.2	2.1
r.m.s. deviation from ideal dihedral angles (°)	27.3	27.9
r.m.s. deviation from ideal improper angles (°)	0.6	1.0

[a] $R_{merge} = \Sigma|I_i - \langle I_i\rangle|/\Sigma|\langle I_i\rangle|$, where I_i is the intensity measurement for reflection *i*, and $\langle I_i\rangle$ is the mean intensity calculated for reflection *i* from replicate data.

[b] $R = \Sigma||F_o| - |F_o||/\Sigma|F_o|$. *R* and R_{free} are calculated using the working and test reflection sets, respectively.

Crystallization and Structure Determination—Crystals of sEH were prepared as described (8), and the sEH-CDU and sEH-CIU complexes were prepared in crystal soaking experiments. Briefly, CDU and CIU were dissolved to concentrations of 100 mM in 100% ethanol and Me_2SO, respectively. 1 μl of each stock solution was added in sitting drop wells containing 100 μl of mother liquor. The sEH crystals were transferred to these wells and soaked in the 1 mM inhibitor solution for 4 days. Crystals were flash-cooled following the addition of 30% glycerol to the mother liquor (v/v).

Diffraction data were collected at Cornell High Energy Synchrotron Source at a wavelength of 0.890 Å at 100 K. Diffraction intensities were measurable to 3.0–3.1 Å resolution. Crystals of each complex were isomorphous with those of the native enzyme and belong to spacegroup $P2_12_12$, a = 151.9 Å, b = 143.0 Å, c = 60.0 Å. Data reduction and integration was achieved with DENZO and SCALEPACK (21). Initial $|F_o| - |F_c|$ and $2|F_o| - |F_c|$ electron density maps were generated with structure factors calculated from the native sEH structure using routines in CCP4 and X-PLOR (22, 23). Initial refinement was achieved with X-PLOR (23). After positional refinement, simulated annealing minimizations (T_{inital} = 3000 K), and individual B factor refinement, both inhibitors were modeled into unbiased $|F_o| - |F_c|$ electron density

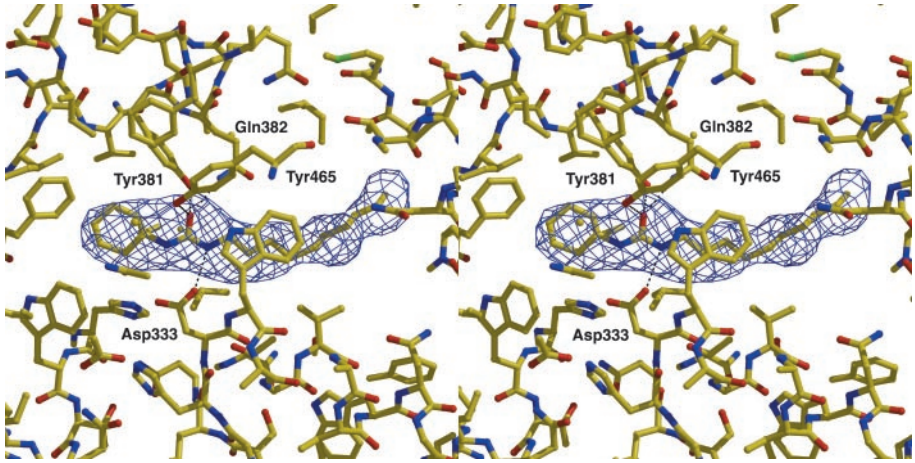

FIG. 3. **Omit electron density map (contoured at 2.5 σ) of the complex between sEH and the competitive inhibitor CDU (K_i = 6.3 ± 0.5 nM).** Residues involved in enzyme-inhibitor hydrogen bonds are indicated. The figure was prepared with BOBSCRIPT and RASTER3D (29–31).

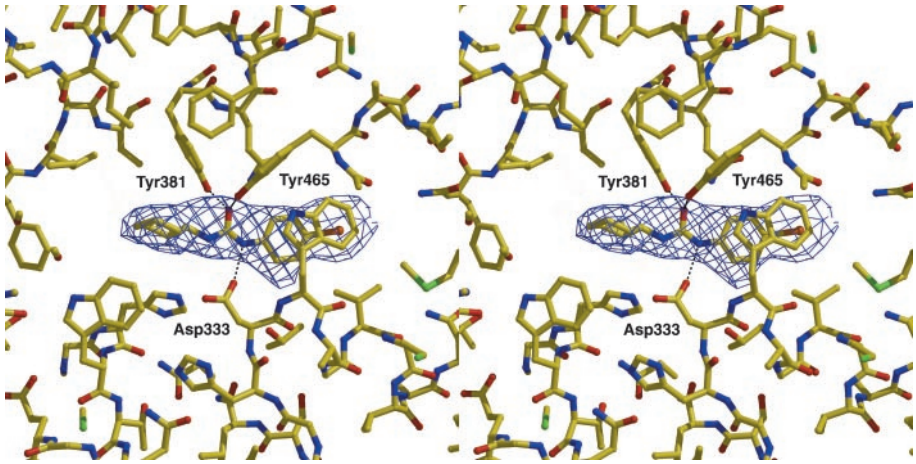

FIG. 4. **Omit electron density map (contoured at 2.5 σ) of the complex between sEH and the competitive inhibitor CIU (K_i = 17 ± 4 nM).** Residues involved in enzyme-inhibitor hydrogen bonds are indicated. The figure was prepared with BOBSCRIPT and RASTER3D (29–31).

using the program O (24). Inhibitor molecules were created, and their conformations were energy-minimized using the program INSIGHT (25). In the last cycles of refinement, waters were added using WATPEAK (22), and their positions were refined with X-PLOR (23). Both inhibitors were bound to the C-terminal domains of each monomer. As in the native structure, the N-terminal Met^{1}–Leu^{3} and the C-terminal Val^{545}–Ile^{554} segments were not modeled because of disorder in both monomers; additionally, Ala^{20}–Glu^{47} and Val^{64}–Ser^{89} were disordered in monomer A. Refinement statistics are recorded in Table I.

RESULTS AND DISCUSSION

Although the resolution of these enzyme-inhibitor complexes is considered modest at 3.0–3.1 Å, the information content of these structures is nevertheless quite high. The binding conformations of CDU and CIU are determined unambiguously, and these conformations are quite similar; that similar conformations are observed in two independent experiments with two independent inhibitors strengthens the interpretation of intermolecular interactions despite the modest resolution. Importantly, the intermolecular interactions of CDU and CIU provide the first glimpse of a constellation of hydrogen bonds that activate epoxide substrates for hydrolysis, and these interactions were not observed in the previously determined structure of the sEH-CPU complex (8). The discussion below outlines the structures of the sEH-CDU and sEH-CIU complexes and then incorporates this new structural information into a brief discussion of substrate specificity and a proposed mechanism for the hydrolysis of complex epoxide substrates.

Inhibitor Binding Modes—The binding of CDU does not trigger any significant tertiary or quaternary structural changes in sEH, as indicated by the r.m.s. deviation of 0.4 Å for 994 Cα atoms between the native enzyme and the enzyme-inhibitor complex. However, some local structural changes are observed in the active site that may reflect possible binding interactions of larger epoxide substrates such as the leukotoxins. The inhibitor binds with a *trans,trans* dialkyl urea linkage, and the *N′*-decyl tail extends out of the active site and makes numerous van der Waals' contacts with hydrophobic residues such as Met^{361}, Val^{372}, Trp^{334}, Val^{337}, and Pro^{363} (Fig. 3). Thermal B factors increase toward the end of the decyl tail of CDU, which may indicate increased flexibility in substrate binding toward the end of the active site tunnel. The *N*-cyclohexyl group packs in the hydrophobic pocket and makes numerous van der Waals' contacts with hydrophobic residues Val^{497}, Phe^{406}, Phe^{265}, Trp^{524}, and Tyr^{381}.

Significantly, the urea carbonyl group accepts hydrogen bonds from Tyr^{465} and Tyr^{381}. Tyr^{465} is a conserved residue in the epoxide hydrolase family and is a proposed general acid in catalysis (8, 17). Although Tyr^{381} is not conserved in the microsomal epoxide hydrolases, it is also considered a possible general acid catalyst (8, 17). Recent experiments show that mutation of Tyr^{381} and Tyr^{465} to phenylalanine individually and together dramatically reduces catalytic activity, particularly with chemically stable substrates; notably, catalytic activity in the double variant is completely eliminated.[2] Likewise, site-directed mutagenesis studies of the epoxide hydrolase from *A. radiobacter* AD1 indicate that both of the corresponding tyrosine residues are important for catalysis (26). Therefore, both x-ray crystallography and site-directed mutagenesis together indicate that Tyr^{381} and Tyr^{465} serve as general acid catalysts that activate the substrate epoxide ring for nucleo-

[2] T. Yamada, C. H. Morisseau, J. E. Maxwell, M. A. Argiriadi, D. W. Christianson, and B. D. Hammock, submitted for publication.

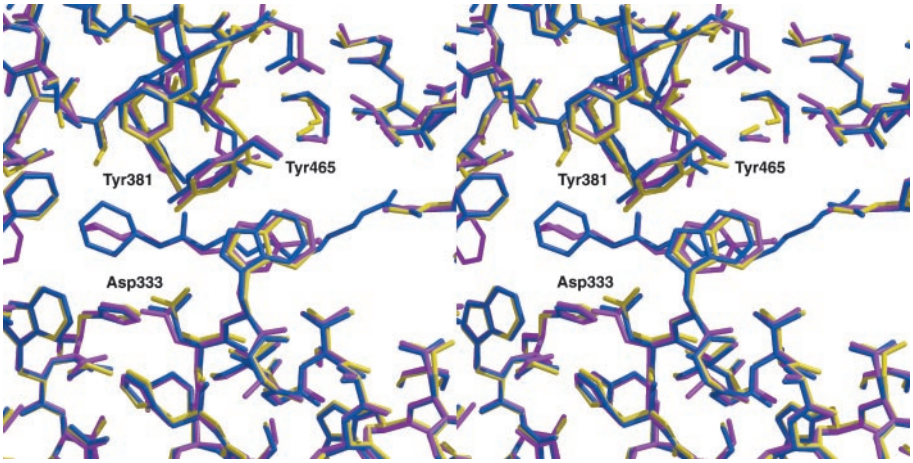

FIG. 5. **Superposition of sEH-CDU and sEH-CIU complexes.** Native sEH is *yellow*, the sEH-CDU complex is *blue*, and the sEH-CIU complex is *magenta*. The figure was prepared with BOBSCRIPT and RASTER3D (29–31).

philic atack by Asp^{333}. Interestingly, Asp^{333} accepts a hydrogen bond from the urea NH group of CDU, which may mimic the interaction between the catalytic nucleophile and the partial positive charge on the substrate epoxide carbon.

Another polar active site residue may play a role in the hydrolysis reaction. The side chain of Gln^{382} undergoes a conformational change and moves closer to the bound inhibitor, donating an additional hydrogen bond to the urea carbonyl group. Because Gln^{382} is conserved among the mammalian isozymes, it is possible that this residue is an electrostatic catalyst that helps to stabilize the epoxide oxygen in catalysis by hydrogen bonding.

As in the sEH-CDU complex, the binding of CIU does not trigger any major tertiary or quaternary structural changes in sEH, as indicated by the r.m.s deviation of 0.5 Å for 994 Cα atoms between the native enzyme and the enzyme-inhibitor complex. Nevertheless, some local structural changes in the active site accommodate inhibitor binding. The inhibitor binds with a *trans,trans*-dialkyl linkage, and the cyclohexyl ring packs in the hydrophobic pocket, making van der Waals' contacts with Val^{497}, Phe^{406}, Phe^{265}, Trp^{524}, and Tyr^{381} (Fig. 4). Interestingly, the cyclohexyl ring of CIU adopts a different conformation with respect to the urea group, corresponding to a 58° rotation about the C-N linkage; this is visible in the superposition of Fig. 5. This reflects the large size of the hydrophobic pocket that can accommodate large substrate substituents and different conformations of such substituents in this region of the active site. The iodophenyl group of CIU binds in the hydrophobic channel, making van der Waals' contacts with Trp^{334}, Leu^{498}, Met^{361}, and Val^{337} (Fig. 4). Because both CDU and CIU bind with *trans*,*trans*-dialkylurea linkages and CPU binds with an unusual *trans*,*cis*-dialkylurea linkage (8), we advance that the binding mode of CPU is probably exceptional and not preferential for this series of inhibitors (7).

There is no indication of "backwards" binding of the inhibitor, because the position of the inhibitor iodine atom in each catalytic domain is confirmed by 12 σ peaks in omit electron density maps (data not shown). As observed in the sEH-CDU complex, the carbonyl group of CIU accepts hydrogen bonds from Tyr^{465} and Tyr^{381}; however, it does not interact with Gln^{382}, even though Gln^{382} undergoes a small conformational change. Finally, Asp^{333} accepts a hydrogen bond from the urea NH group of CIU. The common binding modes of both inhibitors in the sEH active site are clearly visible in the superposition of Fig. 5.

Structural Inferences on Substrate Specificity—With only three or four intermolecular hydrogen bond interactions made in each enzyme-inhibitor complex, the substrate binding conformation is mostly governed by van der Waals' contacts made

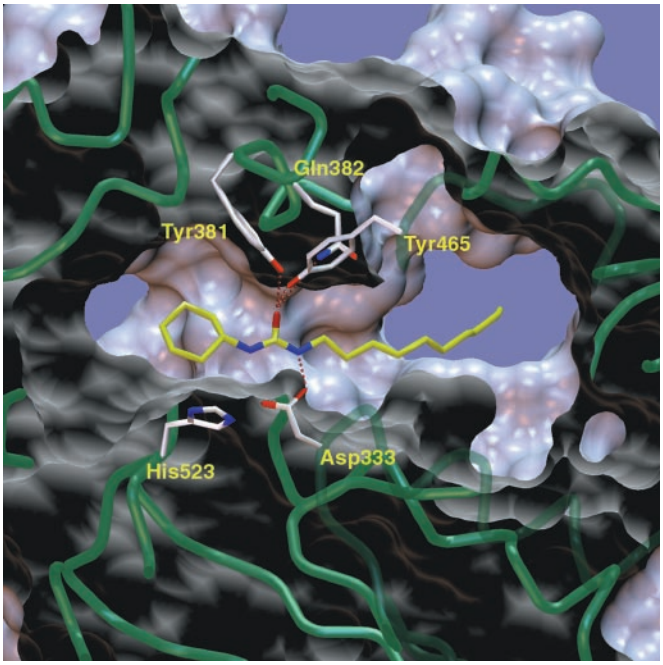

FIG. 6. **A surface representation of the sEH-CDU complex.** Hydrogen bond interactions are indicated between Asp^{333} and the urea NH group and between Tyr^{381}, Gln^{382}, Tyr^{465}, and the urea carbonyl group. The figure was prepared with AVS (32).

with the residues defining the unique active site contour. The binding modes of CDU and CIU show how sEH accommodates large aliphatic substrates such as the leukotoxins. As mentioned previously, the active site is in the middle of a hydrophobic, L-shaped tunnel. The long, aliphatic inhibitor CDU conforms to this hydrophobic L-shaped contour, and corresponding substrate binding modes can be postulated based on the structure of the sEH-CDU complex (Fig. 6). The specificity of sEH will be greatest toward the larger aliphatic substrates that can achieve favorable binding conformation in the L-shaped tunnel; presumably, substrate binding modes in which epoxide substituents dangle out of one end of the active site tunnel would be disfavored.

Introduction of multiple degrees of unsaturation in the substrate can possibly hinder substrate binding, or may alter regiochemical preferences for the nucleophilic attack of Asp^{333} at one or the other epoxide carbon. For example, in the hydrolysis of *cis*-epoxyeicosatrienoic acids, optimal sEH activity favors the 14(*R*),15(*S*)-epoxide rather than the 14(*S*),15(*R*) stereoisomer or the 5,6-, 8,9-, or 11,12-epoxide isomers (27, 28).

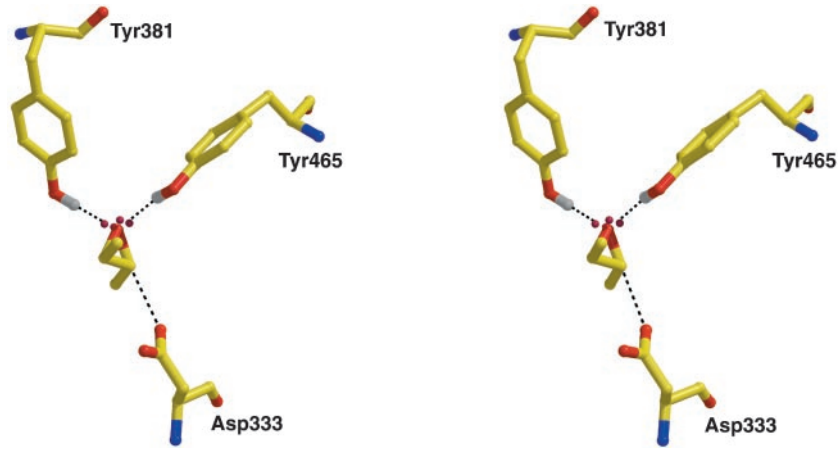

FIG. 7. **Key interactions between Tyr^{465}, Tyr^{381}, Asp^{333}, and an epoxide substrate define the reaction coordinate of the first step of sEH catalysis.** These interactions are based on corresponding hydrogen bonds observed in the sEH-CDU and sEH-CIU complexes. Note that the phenolic OH groups of both tyrosines point directly toward lone electron pairs on the epoxide oxygen. These interactions orient one epoxide carbon for optimal backside attack by the aspartate nucleophile. The figure was prepared with BOBSCRIPT and RASTER3D (29–31).

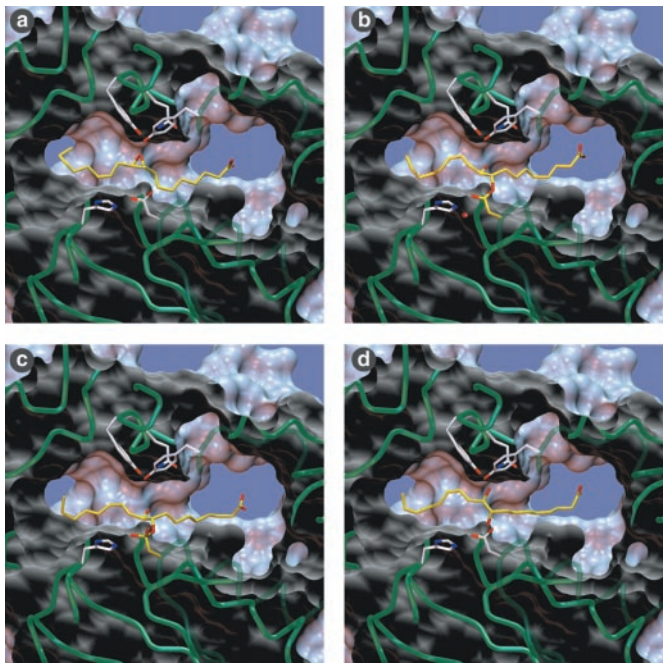

FIG. 8. **Structure-based mechanism for activation and hydrolysis of leukotoxin.** *a*, nucleophilic attack of Asp^{333} yields the alkylenzyme ester intermediate (*b*), which is subsequently attacked by a water molecule (*small red sphere*) through the assistance of general base His^{523}. Collapse of the resulting tetrahedral intermediate (*c*) yields the vicinal leukotoxin diol product (*d*). The figure was prepared with AVS (32).

The *cis*-epoxyeicosatrienoic acids have significant conformational restraints imposed upon binding because of their unsaturation. Apparently, only the 14(*R*),15(*S*)-epoxide isomer can achieve an optimal substrate binding conformation in the L-shaped active site tunnel of sEH. Moreover, preferential formation of the *vic*-dihydroxyeicosatrienoic acid product with 14(*R*),15(*R*) stereochemistry indicates a regiochemical preference for nucleophilic attack of Asp^{333} at C-15 of the 14(*R*),15(*S*)-*cis*-epoxyeicosatrienoic acid substrate (27, 28).

Mechanistic Inferences from Inhibitor Binding—Previous structural and biochemical evidence suggest that sEH catalysis proceeds through an S_N2-like reaction at the substrate epoxide carbon (8, 14–16). The epoxide moiety displays partial positive charges on each carbon and a partial negative charge on the oxygen, and the distribution of partial charge in the reaction coordinate of epoxide ring opening is mimicked by the dialkylurea inhibitors CDU and CIU (Fig. 2). From the hydrogen bond interactions observed in the sEH-CDU and sEH-CIU complexes it is inferred that the carboxylate group of Asp^{333} performs a backside nucleophilic attack on the electrophilic epoxide carbon in concert with proton donation to the epoxide oxygen by Tyr^{465} or Tyr^{381}. Each tyrosine hydroxyl group is oriented nearly perfectly in-line with a lone electron pair on the epoxide oxygen when the epoxide is aligned for nucleophilic attack by Asp^{333} (Fig. 7). Therefore, the constellation of interactions with Asp^{333}, Tyr^{465}, and Tyr^{381} define the reaction coordinate of the first step of catalysis. Possible hydrogen bond interactions with Gln^{382} may mimic additional polar interactions that stabilize the transition state.

In conclusion, the mechanism of leukotoxin hydrolysis outlined in Fig. 8 incorporates the new structural information emanating from the sEH-CDU and sEH-CIU complexes, and this mechanism is representative for the hydrolysis of a lipid epoxide substrate. The carboxylate side chain of Asp^{333} is the catalytic nucleophile that attacks the electrophilic carbon of the epoxide. Directly across the active site cavity from Asp^{333} are the phenolic side chains of Tyr^{465} and Tyr^{381}, one of which can serve as a proton donor to activate and accelerate epoxide ring opening. The tyrosine that does not donate its proton can nevertheless serve as an electrostatic catalyst, along with Gln^{382}, by hydrogen bond donation to the epoxide oxygen. Parenthetically, we note that Tyr^{465} is flanked by edge-to-face interactions with Trp^{334} and Phe^{385} that would stabilize the intermediate phenolate anion; no such interactions can be achieved by the phenolate anion of Tyr^{381}, but this does not rule out Tyr^{381} as a proton donor. The alkylenzyme ester intermediate is subsequently hydrolyzed by a water molecule promoted by general base His^{523}. The basicity of His^{523} is likely enhanced by the negatively charged carboxylate side chain of Asp^{495} and the partial negative charge of the indole ring of Trp^{524}; the imidazole ring makes a classic cation-π interaction with Trp^{524}. Finally, an "oxyanion hole" containing backbone NH groups of Phe^{265} and Trp^{334} may stabilize the oxyanion of the tetrahedral intermediate in alkylenzyme hydrolysis and collapse of this intermediate yields the product leukotoxin diol.

Acknowledgments—We are grateful to the Cornell High Energy Synchrotron Source for beamtime access and to Dr. A. Daniel Jones (Pennsylvania State University) for performing the mass spectral analyses.

REFERENCES

1. Oesch, F. (1973) *Xenobiotica* **3,** 305–340
2. Beetham, J. K., Grant, D., Arand, M., Garbarino, J., Kiyosue, T., Pinot, F., Oesch, F., Belknap, W. R., Shinozaki, K., and Hammock, B. D. (1995) *DNA Cell Biol.* **14,** 61–71
3. Wixtrom, R. N., and Hammock, B. D. (1985) in *Biochemical Pharmacology and Toxicology* (D. Zakim, D. A. Vessey, Eds.) Vol. 1, pp. 1–93, John Wiley & Sons, Inc., New York
4. Ota, K., and Hammock, B. D. (1980) *Science* **207,** 1479–1481
5. Moghaddam, M. F., Grant, D. F., Cheek, J. M., Greene, J. F., Williamson, K. C., and Hammock, B. D. (1997) *Nat. Med.* **3,** 562–566
6. Ishizaki, T., Shigemori, K., Nakai, T., Miyabo, S., Ozawa, T., Chang, S. W., and Voelkel, N. F. (1995) *Am. J. Physiol.* **269,** L65–L70

7. Morisseau, C., Goodrow, M., Dowdy, D., Zheng, J., Greene, J. F., Sanborn, J. R., and Hammock, B. D. (1999) *Proc. Natl. Acad. Sci. U. S. A.* **96,** 8849–8854
8. Argiriadi, M., Morisseau, C., Hammock, B. D., and Christianson, D. W. (1999) *Proc. Natl. Acad. Sci. U. S. A.* **96,** 10637–10642
9. Ollis, D. L., Cheah, E., Cygler, M., Dijkstra, Frolow, F., Franken, S. M., Harel, M., Remington, S. J., Silman, I., Schrag, J., Sussman, J. L., Verschueren, K. H. G., and Goldman, A. (1992) *Protein Eng.* **5,** 197–211
10. Heikinheimo, P., Goldman, A., Jeffries, C., and Ollis, D. L. (1999) *Structure* **7,** R141–R146
11. Franken, S. M., Rozeboom, H. J., Kalk, K. H., and Dijkstra, B. W. (1991) *EMBO J.* **10,** 1297–1302
12. Verschueren, K. H. G., Franken, S. H., Rozeboom, H. J., Kalk, K. H., and Dijkstra, B. W. (1993) *J. Mol. Biol.* **232,** 856–872
13. Verschueren, K. H. G., Seljée, F., Rozeboom, H. J., Kalk, K. H, and Dijkstra, B. W. (1993) *Nature* **363,** 693–698
14. Borhan, B., Jones, A. D., Pinot, F., Grant, D. F., Kurth, M. J., and Hammock, B. D. (1995) *J. Biol. Chem.* **270,** 26923–26930
15. Pinot, F., Grant, D. F., Beetham, J. K., Parker, A. G., Borhan, B., Landt, S., Jones, A. D., and Hammock, B. D. (1995) *J. Biol. Chem.* **270,** 7698–7974
16. Arand, M., Wagner, H., and Oesch, F. (1996) *J. Biol. Chem.* **271,** 4223–4229
17. Nardini, M., Ridder, I. S., Rozeboom, H. J., Kalk, K. H., Rink, R. Janssen, D. B., and Dijkstra, B. W. (1999) *J. Biol. Chem.* **274,** 14579–14586
18. Hisano, T., Hata, Y., Fujii, T., Liu, J.-Q., Kurihara, T., Esaki, N., and Soda, K. (1996) *J. Biol. Chem.* **271,** 20322–20330
19. Ridder, I. S., Rozeboom, H. J., Kalk, K. H., Janssen, D. B., and Dijkstra, B. W. (1997) *J. Biol. Chem.* **272,** 33015–33022
20. Zou, J., Hallberg, B. M., Bergfors, T., Oesch, F., Arand, N., Mowbray, S. L., and Jones, T. A. (2000) *Structure* **8,** 111–122
21. Otwinowski, Z., and Minor, W. (1997) *Methods Enzymol.* **276,** 307–326
22. Collaborative Computational Project, Number 4. (1994) *Acta Crystallogr. Sect. D Biol. Crystallogr.* **50,** 760–763
23. Brünger, A. T., Kuriyan, J., and Karplus, M. (1987) *Science* **235,** 458–460
24. Jones, T. A., Zou, J-Y., Cowan, S. W., and Kjeldgaard, M. (1991) *Acta Crystallogr. Sect. A* **47,** 110–119
25. *Insight II User Guide* (1993) version 2.3.0, Biosym Technologies, San Diego, CA
26. Rink, R., Spelberg, J. H. L., Pieters, R. J., Kingma, J., Nardini, M., Kellogg, R. M., Dijkstra, B. W., and Janssen, D. B. (1999) *J. Am. Chem. Soc.* **121,** 7417–7418
27. Zeldin, D. C., Kobayashi, J., Falck, J. R., Winder, B. S., Hammock, B. D., Snapper, J. R., and Capdevila, J. H. (1992) *J. Biol. Chem.* **268,** 6402–6407
28. Zeldin, D. C., Wei, S., Falck, J. R., Hammock, B. D., Snapper, J. R., and Capdevila, J. H. (1995) *Arch. Biochem. Biophys.* **316,** 443–451
29. Esnouf, R. M. (1997) *J. Mol. Graphics* **15,** 132–134
30. Bacon, D. J., and Anderson, W. F. (1998) *J. Mol. Graph.* **6,** 219–220
31. Merritt, E. A., and Murphy, M. E. P. (1994) *Acta Crystallogr. Sect. D Biol. Crystallogr.* **50,** 869–873
32. Upson, C., Faulhaber, T. J., Kamins, D., Laidlaw, D., Schlegel, D., Vroom, J., Gurwitz, R., and van Dam, A. (1989) *IEEE Comput. Graphics Appl.* **9,** 30–42